Rock and Soil Mechanics

Volume 41 | Issue 1 Article 9

9-23-2020

Horizontal vibration response analysis of piles in liquefied soil under Winkler foundation model

XIONG Hui

YANG Feng

Rock and Soil Mechanics 2020 41(1): 103−110 ISSN 1000−7598
https: //doi.org/10.16285/j.rsm.2018.7332 rocksoilmech.researchcommons.org/journal

Horizontal vibration response analysis of piles in liquefied soil under Winkler foundation model

XIONG Hui, YANG Feng
School of Civil Engineering, Hunan University, Changsha, Hunan 410082, China

Abstract: By considering the condition of vertical load, the soil after complete liquefaction is regarded as fluid, and the pile foundation is equivalent to the Euler-Bernoulli beam model. The vibration impedance of the top of the pile foundation embedded in the pile bottom is discussed. Simulating liquefied soil using fluid dynamic equation and simulating lower non-liquefied soil layer with Winkler foundation, combined with the continuous conditions of displacement, rotation angle and internal force at the interface between the liquefied soil and the non-liquefied soil, the relationship between displacement and internal force expression of pile's top and pile's bottom is obtained by means of the matrix transfer method. Finally, according to the embedded conditions at the bottom of the end bearing pile, the expression of the impedance of the pile's top is obtained. Compared with the existing literature, the correctness of the paper is verified. The parameter analysis of the impedance influence conditions shows that the liquefaction depth, the pile's top axial force and the fluid density have different effects on the impedance of the pile's top.

Keywords: liquefied soil; fluid; Winkler foundation; horizontal vibration

1 Introduction

In 1995, an earthquake struck in Hanshin, Japan, pile foundations were subsided, cracked, and damaged due to liquefaction of the soil, which caused extensive damage to the superstructure, resulting in economic losses of more than $ 10 billion. Since the new century, soil liquefaction caused by the Indian Ocean earthquake and Wenchuan earthquake have also resulted in the destruction of many infrastructures. With the in-depth investigation and research on the seismic damage of pile foundations under the condition of liquefied soil, it has been found that pile foundations are often damaged by earthquakes in liquefaction sites and cause serious loss of life and property. Therefore, scholars conducted research on the seismic performance of pile foundations in liquefied soil, and achieved a series of useful results.

Based on different research methods, the seismic performance of pile foundations in liquefied soil layers can be divided into the following aspects: model test approach, *p-y* curve approach, and finite element and theoretical analysis. Rollins et al.[1] carried out group pile tests at the liquefaction site using transient blasting methods to study the liquefaction characteristics of sand. By conducting shaking table test, Feng et al.[2] calculated the bearing capacity of the pile foundation in liquefied soil through reduction of the *p-y* curve. Gaoet et al.[3] systematically summarized the research results of large ground displacement during liquefaction. Ohtomo et al.[4] conducted tests on the effects of lateral expansion caused by liquefaction on pile foundation in soil, and analyzed the effects of lateral expansion caused by liquefaction on the underground structures. Wanget et al.[5] used the p-y curve to analyze the failure process of the pile foundation of the Showa Bridge and the factors affecting the pile foundation caused by sand liquefaction. Tokimatsu et al.[6] used a shaking table test to study the effects of pile dynamic responses, pile material properties, and soil properties on pile-soil interactions. In the area of finite element study, Shao et al.[7] established a finite element analysis model of pile-soil interaction in liquefied soil, and achieved valuable test results.

It is worth noting that although there are many studies on liquefied soil now, most of them still regard liquefied soil as solid foundation and use the strength reduction method[8-9] to explore the performance of liquefied soil. This is inconsistent with the American Society of Civil Engineers' definition of liquefaction, because liquefaction is the process of converting soil from solid to liquid. Under this definition, the properties of the liquefied soil should be similar to that of the fluid, and should not be a solid with reduced strength. According to the earthquake disaster data[10] in Niigata, Hanshin, Wenchuan and many other places, many structural failures are caused by large-scale lateral flow after sand liquefaction, resulting in damage and failure of the pile foundation. Therefore, treating liquefied soil as a fluid has gradually become an important research direction by many scholars. For example: Chen et al.[11] experimentally studied the properties of sand after liquefaction, and determined the relationship between fluid viscosity and shear strain rate. Although Wang et al.[12] analyzed the influence of soil parameters on pile foundation response, their research is only applicable to solids.

In summary, treating the liquefied soil as fluid in research is

Received: 25 December 2018 Revised: 30 April 2019
This work was funded by Program for New Century Excellent Talents in University(NCET−13−190).
First author: XIOG Hui, male, born in 1975, PhD, associate Professor, mainly engaged in the research on structural's resistance to earthquake and interaction of soil-structure. E-mail: 735092992@qq.com

innovative. However, as mentioned above, the research at this stage is only based on limited pioneering experimental tests and finite element simulations, or analytical solutions. In this paper, the upper liquefied soil is regarded as a fluid, and the lower non-liquefied soil is simulated by the Winkler foundation beam model, and the lower soil is layered. The mechanical properties of the pile foundation in the liquefied soil are analyzed under the axial force. It can be known from the literature [11] that the viscosity of liquefied sand decreases with increasing shear strain rate, therefore, its viscosity can be ignored during strong earthquakes. Since the soil layout in this paper is close to the field condition, it can be seen from the comparison of related literatures [13] that the two are more consistent. Therefore, the solution obtained in this paper can provide a reference for pile foundation structures under the action of earthquakes in areas of easily liquified site (such as coastal areas).

2 Calculation model

The movement of the pile foundation when the top soil layer is liquefied is shown in Fig.1. In the figure, N is the axial force of the pile; c_x^i is the damping coefficient of the i-th layer of soil; k_x^i is the stiffness coefficient of the i-th layer of soil. Assume that the upper soil is liquefied soil (fluid) with a thickness of h_1; the lower non-liquefied layered soil (Winkle foundation) has a thickness of h_2, h_3 ..., h_n. The bottom of the pile is a rigid foundation. The pile foundation is an ideal elastic rod, H is the length of the pile, and r_0 is the radius. Ne^{iwt} is the excitation force at the top (w is the excitation frequency; t is the time), the pile foundation and the liquefied soil and the non-liquefied soil are all small deformations during vibration, and the contact surface does not fall off and slip.

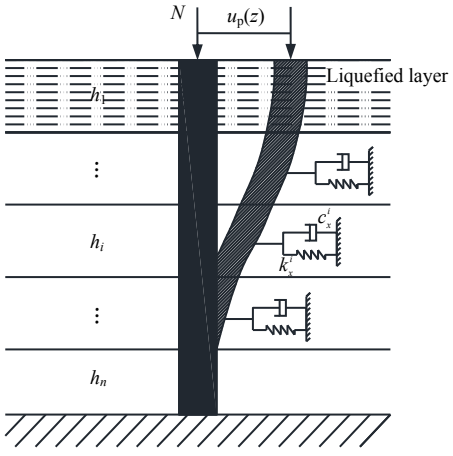

Fig.1 Simplified calculation model

3 Movement of pile foundation in liquefaction layer

3.1 Motion of liquefaction fluid

The soil is simulated as fluid after it is liquefied, the polar coordinate system r, z, and θ is used to do the calculation, and the fluid motion equation is simulated by the Laplace equation:

$$\frac{\partial^2\phi}{\partial r^2}+\frac{1}{r}\frac{\partial\phi}{\partial r}+\frac{1}{r^2}\frac{\partial^2\phi}{\partial\theta^2}+\frac{\partial^2\phi}{\partial z^2}=0 \tag{1}$$

In the above formula: $\phi=\phi(r,\ \theta,\ z,\ t)$ is the potential function when the fluid moves.

Suppose when the liquefaction layer moves it meets the following requirements:

(1) The bottom surface of the liquefaction layer is $z = h_1$, and its vertical velocity is zero, that is:

$$\left.\frac{\partial\phi}{\partial z}\right|_{z=h_1}=0 \tag{2}$$

(2) Ignoring the effect of gravity waves on fluids, in the liquefaction layer, there is:

$$\left.\phi\right|_{z=0}=0 \tag{3}$$

(3) Fluid is stationary at infinity, that is:

$$\left.\phi\right|_{r\to\infty}=0 \tag{4}$$

3.2 Pile's own vibration equation

Assuming a uniform section of the pile, the length of the pile is L, the radius of the pile is r_0, and the bending stiffness of the pile is E_pI_p (in the expression: E_p is the elastic modulus of the pile, I_p is the moment of inertia of the section of the pile), so the differential equation of horizontal vibration of the pile is:

$$E_pI_p\frac{\partial^4u_p(z,t)}{\partial z^4}+m_p\frac{\partial^2u_p(z,t)}{\partial t^2}+N\frac{\partial^2u_p(z,t)}{\partial z^2}+F_l=0 \quad 0\leqslant z<h_1 \tag{5}$$

In the above formula: u_p is the vibration displacement of the soil; m_p is the mass per unit length of the pile; F_l is the flow pressure of the liquefied soil exerted on the pile, and it's expression is:

$$F_l=-\int_0^{2\pi}\rho_l\left.\frac{\partial\phi}{\partial t}\right|_{r=r_0}r_0\cos\theta\mathrm{d}\theta \tag{6}$$

In the above formula: ρ_l is the density of liquefied soil.

4 Solving the partial differential equation

Considering that the pile and fluid soil will eventually be at steady state vibration, the final fluid motion expression can be expressed as: $\phi=\phi(r,\ \theta,\ z)\cdot e^{iwt}$. The final steady-state vibration of the displacement of the pile section can also be expressed as: $u_p(z,\ t)=u_p(z)\cdot e^{iwt}$. Therefore, when performing the equation operation, the e^{iwt} of the two sides can be eliminated. Using the separation variable method and combining the boundary conditions of eqs. (2) to (4), the solution of eq. (1) can be obtained as:

$$\phi=\sum_{j=1}^{\infty}A\mathrm{i}\omega K_1(\mathrm{i}\chi_j r)\cos\theta\mathrm{ch}(\chi_j z) \tag{7}$$

In the above formula: $K_1(\chi_j r)$ is Bessel function; A is the undetermined constant; $\chi_j=(2j\text{-}1)\pi\mathrm{i}/(2h_1)$, $\mathrm{i}=\sqrt{-1}$, $j=1, 2, 3\cdots$

Substituting eq. (7) into eq. (5), we can get the following

https://rocksoilmech.researchcommons.org/journal/vol41/iss1/9
DOI: 10.16285/j.rsm.2018.7332

equation:

$$\frac{\mathrm{d}^4 u_\mathrm{p}(z)}{\mathrm{d}z^4}+\alpha^2\frac{\mathrm{d}^2 u_\mathrm{p}(z)}{\mathrm{d}z^2}-\beta^4 u_\mathrm{p}(z)=-\frac{\pi\rho_l r_0\omega^2}{E_\mathrm{p}I_\mathrm{p}}\sum_{j=1}^{\infty}AK_1(\mathrm{i}\chi_j r_0)\mathrm{ch}(\chi_j z) \tag{8}$$

The calculation formula of α, β is:

$$\alpha^2=\frac{N}{E_\mathrm{p}I_\mathrm{p}},\ \beta^4=\frac{m_\mathrm{p}\omega^2}{E_\mathrm{p}I_\mathrm{p}} \tag{9}$$

Eq. (8) is a fourth-order non-homogeneous differential equation, and the general solution of the homogeneous equation is:

$$u_\mathrm{p}(z)=S_1\sin(\beta_1 z)+S_2\cos(\beta_1 z)+S_3\mathrm{sh}(\beta_2 z)+S_4\mathrm{ch}(\beta_2 z) \tag{10}$$

In the above formula: S_1, S_2, S_3, S_4 are unsolved constants, and there are:

$$\beta_1=\sqrt{\frac{-\alpha^2+\sqrt{\alpha^4+4\beta^4}}{2}},\ \beta_2=\sqrt{\frac{-\alpha^2-\sqrt{\alpha^4+4\beta^4}}{2}} \tag{11}$$

Suppose its special solution is:

$$u_\mathrm{p}^{\#}(z)=\sum_{j=1}^{\infty}AB_j\mathrm{ch}(\chi_j z) \tag{12}$$

Substituting it into eq. (8), we can get:

$$B_j=-\frac{1}{E_\mathrm{p}I_\mathrm{p}}\frac{\pi\rho_l r_0\omega^2 K_1(\mathrm{i}\chi_j r_0)}{\chi_j^{\ 4}+\alpha^2\chi_j^{\ 2}-\beta^4} \tag{13}$$

Then we can get the solution of the equation, that is:

$$u_\mathrm{p}(z)=S_1\sin(\beta_1 z)+S_2\cos(\beta_1 z)+S_3\mathrm{sh}(\beta_2 z)+S_4\mathrm{ch}(\beta_2 z)-\sum_{j=1}^{\infty}\frac{1}{E_\mathrm{p}I_\mathrm{p}}\frac{\pi\rho_l r_0\omega^2 K_1(\mathrm{i}\chi_j r_0)}{\chi_j^{\ 4}+\alpha^2\chi_j^{\ 2}-\beta^4}\mathrm{ch}(\chi_j z)A \tag{14}$$

The velocity of the pile at the surface $r = r_0$ is the same as the velocity of the fluid, thus we can get:

$$\left.\frac{\partial\phi}{\partial r}\right|_{r=r_0}=\frac{\partial u_\mathrm{p}}{\partial t}\cos\theta \tag{15}$$

Substituting it into the corresponding expression, we can get:

$$\left[S_1\sin(\beta_1 z)+S_2\cos(\beta_1 z)+S_3\mathrm{sh}(\beta_2 z)+S_4\mathrm{ch}(\beta_2 z)-\sum_{j=1}^{\infty}\frac{1}{E_\mathrm{p}I_\mathrm{p}}\frac{\pi\rho_l r_0\omega^2 K_1(\mathrm{i}\chi_j r_0)}{\chi_j^{\ 4}+\alpha^2\chi_j^{\ 2}-\beta^4}\mathrm{ch}(\chi_j z)A\right]\cdot \mathrm{i}\omega\cos\theta=\sum_{j=1}^{\infty}\left[K_1(\mathrm{i}\chi_j r_0)\right]'\cos\theta\,\mathrm{ch}(\chi_j z)\mathrm{i}\omega A \tag{16}$$

In the formula: $[K_1(\mathrm{i}\chi_j r_0)]'$ is the derivative of $K_1(\mathrm{i}\chi_j r_0)$ for r, then take $r = r_0$, because the hyperbolic cosine function is an orthogonal function system on the interval $[0, h_1]$, it is satisfied with:

$$\int_0^{h_1}\mathrm{ch}(\chi_j z)\mathrm{ch}(\chi_j z)\mathrm{d}z=\begin{cases}h_1/2, & i=j\\ 0, & i\neq j\end{cases} \tag{17}$$

Multiply eq. (17) in the interval [0, h1] by ch($\chi_j z$), and then integrate over $[0, h_1]$ to get

$$A=\frac{N_1S_1+N_2S_2+N_3S_3+N_4S_4}{\frac{h_1}{2}\left\{\frac{\pi\rho_l r_0\omega^2K_1(\mathrm{i}\chi_j r_0)}{E_\mathrm{p}I_\mathrm{p}(\chi_j^4+\alpha^2\chi_j^2-\beta^4)}+\left[K_1(\mathrm{i}\chi_j r_0)\right]'\right\}} \tag{18}$$

In the above formula:

$$N_1=\int_0^{h_1}\sin(\beta_1 z)\mathrm{ch}(\chi_j z)\mathrm{d}z \tag{19}$$

$$N_2=\int_0^{h_1}\cos(\beta_1 z)\mathrm{ch}(\chi_j z)\mathrm{d}z \tag{20}$$

$$N_3=\int_0^{h_1}\mathrm{sh}(\beta_2 z)\mathrm{ch}(\chi_j z)\mathrm{d}z \tag{21}$$

$$N_4=\int_0^{h_1}\mathrm{ch}(\beta_2 z)\mathrm{ch}(\chi_j z)\mathrm{d}z \tag{22}$$

By integrating the constant terms, the solution of the homogeneous equation can be obtained as:

$$\begin{aligned}u_\mathrm{p}(z)=&S_1\left[\sin(\beta_1 z)-\sum_{j=1}^{\infty}\eta_1\mathrm{ch}(\chi_j z)\right]+\\ &S_2\left[\cos(\beta_1 z)-\sum_{j=1}^{\infty}\eta_2\mathrm{ch}(\chi_j z)\right]+\\ &S_3\left[\mathrm{sh}(\beta_2 z)-\sum_{j=1}^{\infty}\eta_3\mathrm{ch}(\chi_j z)\right]+\\ &S_4\left[\mathrm{ch}(\beta_2 z)-\sum_{j=1}^{\infty}\eta_4\mathrm{ch}(\alpha\chi_j z)\right]\end{aligned} \tag{23}$$

In the above formula:

$$\left.\begin{aligned}\eta_1&=\kappa N_1\\ \eta_2&=\kappa N_2\\ \eta_3&=\kappa N_3\\ \eta_4&=\kappa N_4\end{aligned}\right\} \tag{24}$$

$$\kappa=\frac{2\pi\rho_l r_0\omega^2K_1(\mathrm{i}\alpha_j r_0)}{h_1\left\{\pi\rho_l r_0\omega^2K_1(\mathrm{i}\chi_j r_0)+\left[K_1(\mathrm{i}\chi_j r_0)\right]'(\chi_j^4+\alpha^2\chi_j^2-\beta^4)E_\mathrm{p}I_\mathrm{p}\right\}} \tag{25}$$

Then from the Euler Bernoulli beam model, combined with relevant knowledge in material mechanics, it can be known that the displacement u, the angle of rotation φ, the bending moment M, and the shear force Q satisfy the following relations:

$$\begin{bmatrix}u\\ \varphi\\ \dfrac{M}{E_\mathrm{p}I_\mathrm{p}}\\ \dfrac{Q}{E_\mathrm{p}I_\mathrm{p}}\end{bmatrix}=\left[T_1(z)\right]\begin{bmatrix}S_1\\ S_2\\ S_3\\ S_4\end{bmatrix} \tag{26}$$

In the above formula:

$$\left[T_1(z)\right]=\left[\boldsymbol{I}_1\ \ \boldsymbol{I}_2\ \ \boldsymbol{I}_3\ \ \boldsymbol{I}_4\right] \tag{27}$$

$$\boldsymbol{I}_1=\begin{bmatrix}\sin(\beta_1 z)-\sum_{j=1}^{\infty}\eta_1\mathrm{ch}(\chi_j z)\\ \beta_1\cos(\beta_1 z)-\sum_{j=1}^{\infty}\eta_1\chi_j\mathrm{sh}(\chi_j z)\\ -\beta_1^2\sin(\beta_1 z)-\sum_{j=1}^{\infty}\eta_1\chi_j^2\mathrm{ch}(\chi_j z)\\ -\beta_1^3\cos(\beta_1 z)-\sum_{j=1}^{\infty}\eta_1\chi_j^3\mathrm{sh}(\chi_j z)\end{bmatrix} \tag{28}$$

$$\boldsymbol{I}_2=\begin{bmatrix}\cos(\beta_1 z)-\sum_{j=1}^{\infty}\eta_2\mathrm{ch}(\chi_j z)\\ -\beta_1\sin(\beta_1 z)-\sum_{j=1}^{\infty}\eta_2\chi_j\mathrm{sh}(\chi_j z)\\ -\beta_1^2\cos(\beta_1 z)-\sum_{j=1}^{\infty}\eta_2\chi_j^2\mathrm{ch}(\chi_j z)\\ \beta_1^3\sin(\beta_1 z)-\sum_{j=1}^{\infty}\eta_2\chi_j^3\mathrm{sh}(\chi_j z)\end{bmatrix} \tag{29}$$

$$\boldsymbol{I}_3=\begin{bmatrix}\mathrm{sh}(\beta_2 z)-\sum_{j=1}^{\infty}\eta_3\mathrm{ch}(\chi_j z)\\ \beta_2\mathrm{ch}(\beta_2 z)-\sum_{j=1}^{\infty}\eta_3\chi_j\mathrm{sh}(\chi_j z)\\ \beta_2^2\mathrm{sh}(\beta_2 z)-\sum_{j=1}^{\infty}\eta_3\chi_j^2\mathrm{ch}(\chi_j z)\\ \beta_2^3\mathrm{ch}(\beta_2 z)-\sum_{j=1}^{\infty}\eta_3\chi_j^3\mathrm{sh}(\chi_j z)\end{bmatrix} \tag{30}$$

$$\boldsymbol{I}_4=\begin{bmatrix}\mathrm{ch}(\beta_2 z)-\sum_{j=1}^{\infty}\eta_4\mathrm{ch}(\chi_j z)\\ \beta_2\mathrm{sh}(\beta_2 z)-\sum_{j=1}^{\infty}\eta_4\chi_j\mathrm{sh}(\chi_j z)\\ \beta_2^2\mathrm{ch}(\beta_2 z)-\sum_{j=1}^{\infty}\eta_4\chi_j^2\mathrm{ch}(\chi_j z)\\ \beta_2^3\mathrm{sh}(\beta_2 z)-\sum_{j=1}^{\infty}\eta_4\chi_j^3\mathrm{sh}(\chi_j z)\end{bmatrix} \tag{31}$$

Assume that the displacement, rotation angle, bending moment, and shear force at the top of the pile are $u_1(0)$, $\varphi_1(0)$, $M_1(0)$ and $Q_1(0)$ respectively; the displacement, rotation angle, bending moment, and shear force at the interface of liquefied soil and saturated soil are $u_1(h_1)$, $\varphi_1(h_1)$, $M_1(h_1)$ and $Q_1(h_1)$ respectively; we can get the relationship between displacement and internal force at the top of the pile and the interface at the liquefied soil layer can be derived:

$$\begin{bmatrix}u_1(h_1)\\ \varphi_1(h_1)\\ \dfrac{M_1(h_1)}{E_\mathrm{p}I_\mathrm{p}}\\ \dfrac{Q_1(h_1)}{E_\mathrm{p}I_\mathrm{p}}\end{bmatrix}=\left[T_1(h_1)\right]\left[T_1(0)\right]^{-1}\begin{bmatrix}u_1(0)\\ \varphi_1(0)\\ \dfrac{M_1(0)}{E_\mathrm{p}I_\mathrm{p}}\\ \dfrac{Q_1(0)}{E_\mathrm{p}I_\mathrm{p}}\end{bmatrix} \tag{32}$$

5 Non-liquefied soil layer's vibration equation

The non-liquefied soil layer uses the Winkler foundation beam model, and its vibration equation is:

$$E_\mathrm{p}I_\mathrm{p}\frac{\partial^4 u_\mathrm{p}^i(z,t)}{\partial z^4}+m_\mathrm{p}\frac{\partial^2 u_\mathrm{p}^i(z,t)}{\partial t^2}+N\frac{\partial^2 u_\mathrm{p}^i(z,t)}{\partial z^2}+K_\mathrm{h}^i u_\mathrm{p}^i(z,t)+c_\mathrm{h}^i\frac{\partial u_\mathrm{p}^i(z,t)}{\partial t}=0 \tag{33}$$

The calculation process is referred to literature [14]. The derivation process is briefly shown below, and the results will be used directly.

$$\begin{bmatrix}u_i(h_i)\\ \varphi_i(h_i)\\ \dfrac{M_i(h_i)}{E_\mathrm{p}I_\mathrm{p}}\\ \dfrac{Q_i(h_i)}{E_\mathrm{p}I_\mathrm{p}}\end{bmatrix}=\left[T_i(h_i)\right]\left[T_i(0)\right]^{-1}\begin{bmatrix}u_i(0)\\ \varphi_i(0)\\ \dfrac{M_i(0)}{E_\mathrm{p}I_\mathrm{p}}\\ \dfrac{Q_i(0)}{E_\mathrm{p}I_\mathrm{p}}\end{bmatrix} \tag{34}$$

In the above formula: i =2, 3, 4,……

From the continuous equation at the interface of the soil layer, we know:

$$\begin{aligned}&u_i(0)=u_{i-1}(h_{i-1}),\quad \varphi_i(0)=\varphi_{i-1}(h_{i-1})\\ &M_i(0)=M_{i-1}(h_{i-1}),\quad Q_i(0)=Q_{i-1}(h_{i-1})\end{aligned} \tag{35}$$

Therefore, the following expressions of displacement and internal force of the pile bottom and pile top are derived:

$$\begin{bmatrix}u_n(h_n)\\ \varphi_n(h_n)\\ \dfrac{M_n(h_n)}{E_\mathrm{p}I_\mathrm{p}}\\ \dfrac{Q_n(h_n)}{E_\mathrm{p}I_\mathrm{p}}\end{bmatrix}=\left[T_n\right]\begin{bmatrix}u_1(0)\\ \varphi_1(0)\\ \dfrac{M_1(0)}{E_\mathrm{p}I_\mathrm{p}}\\ \dfrac{Q_1(0)}{E_\mathrm{p}I_\mathrm{p}}\end{bmatrix} \tag{36}$$

In the above formula:

$$\left[T_n\right]=\left[T_n(h_n)\right]\left[T_n(0)\right]^{-1}\left[T_{n-1}(h_{n-1})\right]\left[T_{n-1}(0)\right]^{-1}\cdots\left[T_1(h_1)\right]\left[T_1(0)\right]^{-1} \tag{37}$$

When the pile is an end-bearing pile,

$$u_n(h_n)=0,\ \varphi_n(h_n)=0 \tag{38}$$

Substituting eq. (38) into expression (37), we can get:

$$\begin{bmatrix}\dfrac{M_1(0)}{E_\mathrm{p}I_\mathrm{p}}\\ \dfrac{Q_1(0)}{E_\mathrm{p}I_\mathrm{p}}\end{bmatrix}=K_\mathrm{s}\begin{bmatrix}u_1(0)\\ \varphi_1(0)\end{bmatrix} \tag{39}$$

In the above formula:

$$K_\mathrm{s}=-\begin{bmatrix}T_n(1,3) & T_n(1,4)\\ T_n(2,3) & T_n(2,4)\end{bmatrix}^{-1}\begin{bmatrix}T_n(1,1) & T_n(1,2)\\ T_n(2,1) & T_n(2,2)\end{bmatrix} \tag{40}$$

In the above formula: $T_n(i, j)$ is in the i-th row and j-th

column of the matrix T_n.

Combined with the definition of dynamic impedance, the horizontal impedance can be obtained:

$$K_{\mathrm{h}} = K_{\mathrm{s}}(2,1) \tag{41}$$

Swing impedance is

$$K_{\mathrm{r}} = K_{\mathrm{s}}(1,2) \tag{42}$$

Coupling impedance is

$$K_{\mathrm{hr}} = K_{\mathrm{s}}(1,1) = K_{\mathrm{s}}(2,2) \tag{43}$$

6 Numerical results and discussions

6.1 Literature comparison

The derivation presented in this paper can be validated by the following methods: the thickness of the lower non-liquefied soil is zero, the density of the fluid is taken as the water, and it is regarded as the pile foundation vibrating in water, which can be compared with that in literature [13]. At this time, the pile foundation parameters are taken as follows: H= 15 m, r_0= 0.5 m, ρ_{p}= 2 500 kg / m^3, E_{p}= 2.55×10^{10} Pa, ρ_{w}= 1 000 kg / m^3; (ρ_{p} is the density of the pile body, ρ_{w} is the density of water) The results of the two papers are compared as follows (Fig. 2), which illustrates the correctness of the solution proposed in this paper.

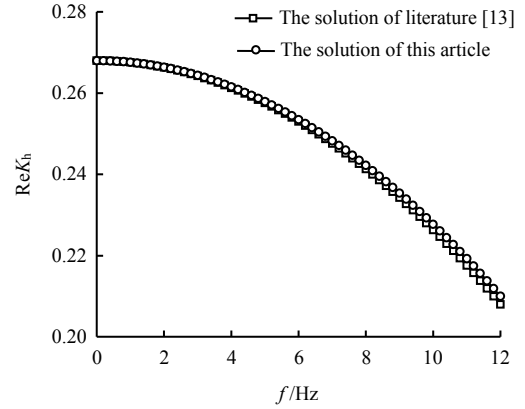

(a) real horizontal impedance

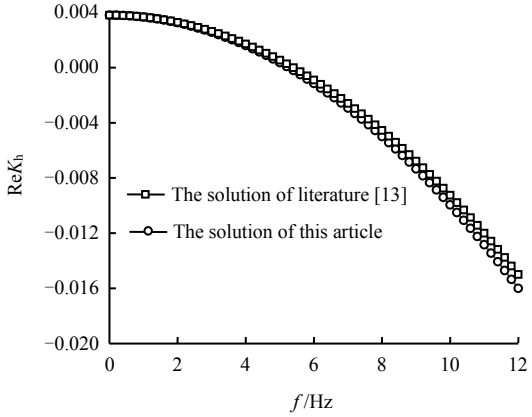

(b) real swing impedance

Fig.2 Comparison of solutions from this paper and literature[13]

6.2 Influence of axial force

The parameters that influence the axial force are shown in Table 1.

Table 1 Axial force influence parameter

Soil layer	Compression modulus E_{si}/MPa	Shear wave velocity V_{si}/(m • s^{-1})	Poisson's ratio υ_i	Damping ratio ξ_i	Density ρ_{si} /(kg • m^{-3})	Thickness of soil /m
1	–	–	–	–	–	5
2	106	125	0.3	0.166	1.9×10^3	5
3	132	165	0.3	0.174	1.95×10^3	5

Fig.3 to 5 show the effect of the axial force on the pile top impedance. As can be seen from the figure: at low frequencies, the axial force has a small effect on the impedance of the pile, but as the frequency increases, the influence of the axial force on the impedance becomes more and more prominent. It reduces the stiffness of the pile significantly but increases damping, but in general, as the axial force increases, the impedance decreases; the increase of the axial force will also reduce the stiffness factor, which will increase the deformation of the pile, therefore, the magnitude of the axial force should be controlled in practice to prevent the pile body deformation and damage.

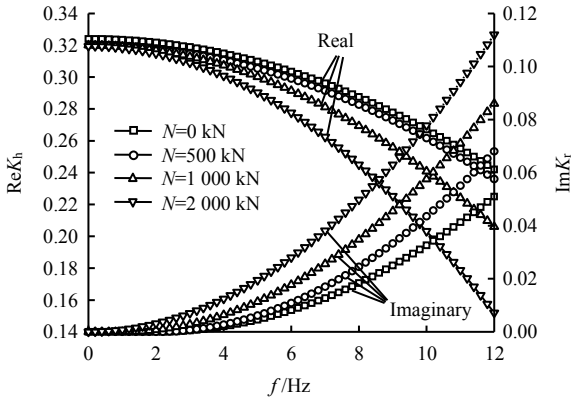

Fig.3 Axial force horizontal impedance factor

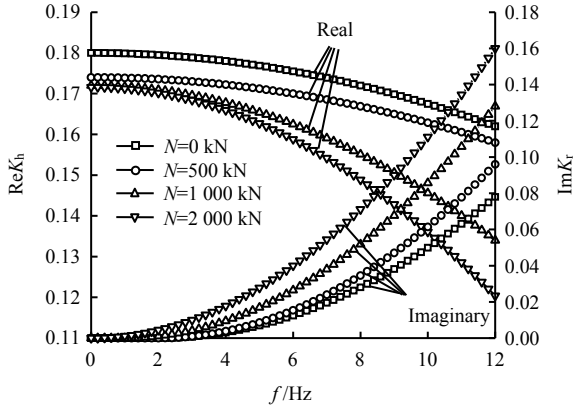

Fig.4 Axial force rocking impedance factor

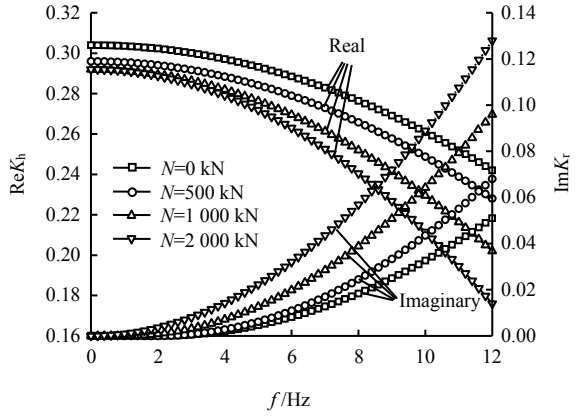

Fig.5 Axial force coupling impedance factor

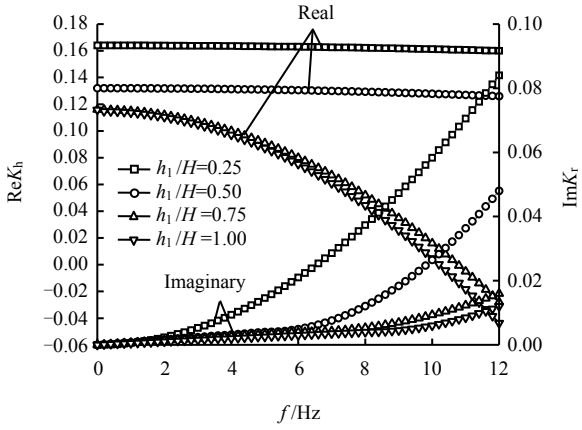

Fig.7 Liquefaction depth rocking impedance factor

6.3 Effect of liquefaction depth

The parameter values that influence the liquefaction depth are shown in Table 2.

Table 2 Liquefaction depth parameters

Soil layer	Compression modulus E_{si}/MPa	Shear wave velocity V_{si}/(m • s^{-1})	Poisson's ratio υ_i	Damping ratio ξ_i	Density ρ_{si} /(kg • m^{-3})	Total thickness /m
lique	–	–	–	–	–	20
no lique	106	125	0.3	0.166	1.9×10^3	

Fig.6 to 8 show the impedance change when the liquefaction depth is different. As shown in the figure, the impedance at the top of the pile decreases as the liquefaction depth increases, and the larger the frequency, the greater the reduction. However, when the liquefaction depth reaches a certain value, the impedance change becomes very small and the damping term is almost zero; when the liquefaction depth is large, the pile top impedance shows negative stiffness at high frequency. Therefore, when designing the site where the soil is easy to liquefy, special attention should be paid to the depth of the liquefaction of the soil.

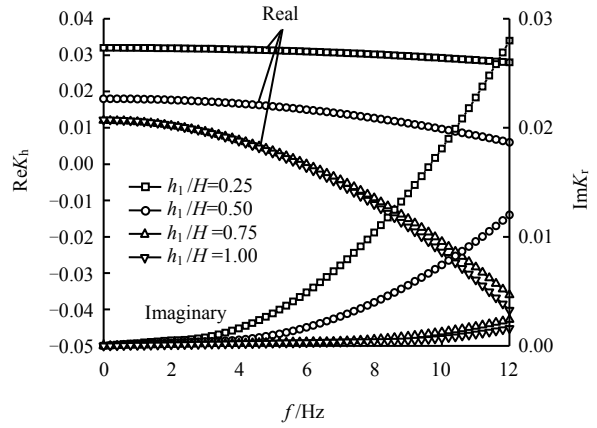

Fig.6 Liquefaction depth horizontal impedance factor

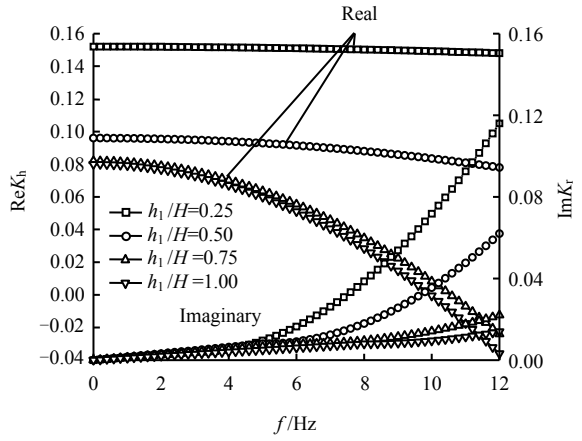

Fig.8 Liquefaction depth coupling impedance factor

6.4 Effect of density of liquefied soil

The parameter values that influence density of the liquefied soil are shown in Table 3.

Table 3 Fluid density parameters

Soil layer	Compression modulus E_{si}/MPa	Shear wave velocity V_{si}/(m • s^{-1})	Poisson's ratio υ_i	Damping ratio ξ_i	Density ρ_{si} /(kg • m^{-3})	Thickness of soil /m
1	–	–	–	–	–	5
2	106	125	0.3	0.166	1.9×10^3	5
3	132	165	0.3	0.174	1.95×10^3	5

Fig.9 to 11 show the effect of fluid density on pile top impedance. As can be seen from the figure, the fluid density has a small effect on the pile top impedance at low frequencies; as the frequency increases, the stiffness decreases with increasing fluid density, but the decline magnitude decreases with increasing fluid density. This is because the high-density fluid has a greater force on the pile body, the stiffness of the pile top is reduced. However, the effect of fluid density on the pile top damping is small, and it can be ignored when the frequency is low.

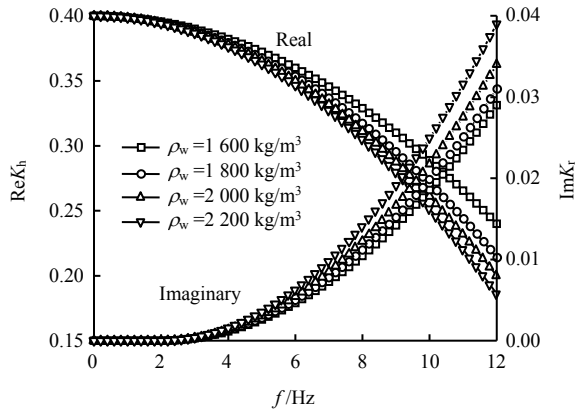

Fig.9 Fluid density horizontal impedance factor

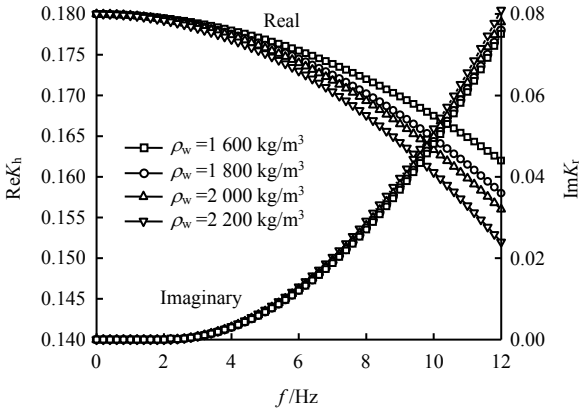

Fig.10 Fluid density rocking impedance factor

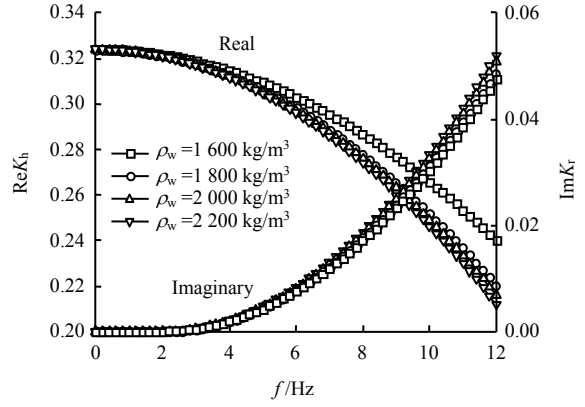

Fig.11 Fluid density coupled impedance factor

7 Conclusions

Figs. 3 to 8 indicate that the real part of impedance of the pile top in the liquefied soil generally decreases as the vibration frequency increases, and the imaginary part of impedance generally increases as the vibration frequency increases. After carrying out a detailed analysis, we come to the following conclusions:

(1) Regarding the liquefied soil as a fluid, adopts the Winkler foundation layered soil model for the non-liquefied soil, combined with boundary conditions and vibration coupling conditions, and using the transfer matrix method, we obtain the analytical solution of the pile top impedance. Numerical simulation is used to verify its correctness. Then, the trend of the impedance of the pile foundation with frequency under different factors is discussed.

(2) In the low frequency range, the axial force has a small effect on the impedance; in the high frequency range, the stiffness decreases and the damping increases as the axial force increases. However, the impedance decreases in general.

(3) As the liquefaction depth increases, the impedance at the top of the pile decreases, and the decrease amplitude increases with increasing frequency. When the liquefaction depth reaches a certain value, the damping is almost zero, and negative stiffness appears in the high frequency range.

(4) At low frequencies, the effect of fluid density on impedance is small; as frequency increases, stiffness decreases with increasing density, but the magnitude decreases with increasing density. Overall, the effect of fluid density on damping is small.

References

[1] ROLLINS K M, GERBER T M, LANE J D, et al. Lateral resistance of a full-scale pile group in liquefied sand[J]. Journal of Geotechnical and Geoenvironmental, 2005, 131(1): 115-125.

[2] FENG Shi-lun, WANG Jian-hua. Shake table test on pile foundation in saturated sand[J]. The Journal of Tianjin University, 2006, 39(8): 951-956.

[3] GAO Yu-feng, LIU Han-long, ZHU Wei. Advances in large ground displacement induced by seismic liquefaction[J]. Rock and Soil Mechanics, 2000, 21(3): 294-298.

[4] OHTOMO K, HAMADA M. Soil force acting on pile in laterally flowing ground by soil liquefaction[C]//The 15th US National Conference on Earthquake Engineering. Chicago: [s. n.], 1994: 241-250.

[5] WANG Rui, ZHANG Jian-min, ZHANG Ga. Analysis of failure of piled foundation due to lateral spreading in liquefied soils[J]. Rock and Soil Mechanics, 2011, 32(1): 501-502.

[6] TOKIMATSU K, SUZUKI H. Pore water pressure response around pile and its effects on *p-y* behavior during soil liquefaction[J]. Soils and Foundations, 2004, 44(6): 53-63.

[7] SHAO Qi. 3D nonlinear analysis of pile-soil interaction in lateral spreading of liquefied ground[D]. Dalian: Dalian University of Technology, 2009.

[8] QIN Shi-wei, MO Long, SHI Hui-zhi. Characteristics of horizontal vibration of end-bearing piles in liquefied soils under axial force[J]. Rock and Soil Mechanics, 2013, 34(4): 987-995.

[9] JIANG Ya-feng. Analysis of vibration characteristics of pile foundation in layered liquefiable soil[D]. Changsha: Hunan University, 2017.

[10] ZHANG Xiao. Numerical analysis of pile foundation failure under lateral movement of earthquake liquefaction site[D]. Jinan: Shandong Jianzhu University, 2014.

[11] CHEN Yu-min, LIU Han-long, ZHOU Yun-dong. Analysis on flow characteristics of liquefied and post-liquefied sand[J]. Chinese Journal of Geotechnical Engineering, 2006, 28(9): 1139-1143.

[12] WANG Teng, DONG Sheng, FENG Xiu-li. Study on influence of soil parameters on lateral response of pile foundations[J]. Rock and Soil Mechanics, 2004, 25(Suppl.): 71-74.

[13] XU Han-zhong. Formula for free vibration frequencies of cantilever cylinder in water[J]. Journal of Hohai University, 1986, 14(4): 10-21.

[14] XIONG Hui. Dynamic interaction analysis and optimization design of upper and lower structures in layered field[D]. Changsha: Hunan University, 2003.